# Single-Crystalline Barium Titanate Nanowires

By *Jeffrey J. Urban, Jonathan E. Spanier, Lian Ouyang, Wan Soo Yun*, and *Hongkun Park**

Single-crystalline barium titanate nanowires are synthesized using a solution-based method, and their ferroelectric properties are investigated by scanning probe microscopy. Pristine nanowires have diameters ranging from 5 to 70 nm and lengths exceeding 10 μm, and they possess perovskite structures with a principal axis aligned along the wire axis. Scanning probe microscopy investigations show that local non-volatile electric polarization can be reproducibly induced and manipulated on nanowires as small as 10 nm in diameter.
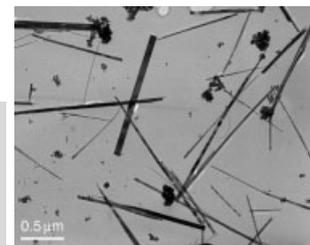
1. Introduction

Over the last decade, low-dimensional nanostructures have received considerable attention from the scientific and engineering communities.[1,2] These structures exhibit distinct properties from bulk materials due to their small size and large surface-to-volume ratios, and they are promising candidates for realizing nanoscale electronic, optical, and mechanical devices. One-dimensional nanostructures, such as nanotubes[2–4] and nanowires,[5–9] represent a particularly attractive class of nanostructures because they can function as both nanoscale device elements and interconnects while retaining unique properties due to size confinement in the radial direction.[2,5,7–9] To date, most research efforts have been directed toward synthesizing carbon nanotubes and semiconductor nanowires,[2–6,10] although experimental strategies that may be applied to other classes of materials are beginning to emerge.[2,11–13]

Ferroelectric oxides, which exhibit a spontaneous electric polarization that can be reoriented by an external electric field, form the basis of ferroelectric non-volatile memory and transistor devices.[14,15] These oxides also exhibit other related properties, including piezoelectricity, pyroelectricity, and large dielectric constants, and they have been used in fabricating microactuators, sensors, and capacitors.[14,15] With the miniaturization trend in device size, the size-dependent evolution of ferroelectricity in thin-film and nanocrystalline samples has

been the focus of much research effort.[15–19] Nanoscale ferroelectric oxides have been shown to exhibit many unique properties, such as size-induced depression of the phase-transition temperature[19] and the emergence of ferroelectricity in antiferroelectric films.[20] Despite intense experimental efforts, however, a clear fundamental understanding of nanoscale ferroelectricity has yet to emerge.

In this research news article, we will briefly summarize a recent experimental development that enables the synthesis and characterization of single-crystalline ferroelectric nanowires. Specifically, we will discuss the synthesis of single-crystalline nanowires composed of barium titanate ($BaTiO_3$), a prototypical displacive ferroelectric material[14,15] that yields well-isolated nanowires with diameters ranging from 5 to 70 nm and lengths reaching up to > 10 μm.[21] These nanowires are composed of single-crystalline $BaTiO_3$ with a principal axis preferentially aligned along the wire axis.[21] We will also discuss scanning probe microscopy investigations where non-volatile electric polarization is reproducibly induced and manipulated on these nanowires by an external electric field.[22] These measurements demonstrate that nanowires remain ferroelectric despite their small radial dimension. Non-volatile polarization domains as small as ~ 100 nm^2 in size can be induced on these nanowires with a retention time exceeding seven days, suggesting that ferroelectric nanowires may be used to fabricate non-volatile memory devices with an integration density approaching 1 terabit cm^{-2}.

2. Synthesis of Barium Titanate Nanowires

Many of prototypical ferroelectric materials, such as $BaTiO_3$ and $PbZr_xTi_{1-x}O_3$ (PZT), possess cubic perovskite struc-

[*]   Prof. H. Park, J. J. Urban, Dr. J. E. Spanier, L. Ouyang, Dr. W. S. Yun[+]
      Department of Chemistry and Chemical Biology
      Harvard University
      Cambridge, MA 02138 (USA)
      E-mail: HPark@chemistry.harvard.edu
[+]   Present Address: Korea Research Institute of Standards and Science,
      Daejeon, Korea.

tures. The synthesis of ternary oxide perovskites has traditionally been accomplished by a wide variety of approaches, including sol–gel[23,24] and vapor deposition.[25,26] Syntheses of well-isolated nanostructures of ferroelectric oxides have been rather scant, however, because the high-temperature heat treatments inherent to these synthetic methods typically cause nanocrystalline particles to lose their small size.

Recently, O'Brien and coworkers and our group have developed a synthetic scheme that produces well-isolated perovskite nanocrystals[27] and nanowires[21] of homogeneous composition. This approach, which is based on the decomposition of bimetallic precursors, produces the correct product stoichiometry and avoids high-temperature treatment steps. Specifically, our synthesis of $BaTiO_3$ nanowires was accomplished by solution-phase decomposition of barium titanium isopropoxide, $BaTi[OCH(CH_3)_2]_6$, in the presence of coordinating ligands, a similar method to that used to prepare metallic and semiconducting nanocrystals and nanowires.[10,11,28] In a typical reaction, an excess of 30 % H_2O_2 was added at 100 °C to a heptadecane solution containing a 10:1 molar ratio of $BaTi[OCH(CH_3)_2]_6$ to oleic acid. The reaction mixture was then subsequently heated to 280 °C for six hours, resulting in a white precipitate composed of nanowire aggregates. Well-isolated nanowires were obtained by sonication of the reaction product followed by fractionation between water and hexane. Elemental analysis shows that the reaction product contains stoichiometric amounts of Ba and Ti.

A representative transmission electron microscope (TEM) image of the reaction product is shown in Figure 1a, and it clearly shows that the reaction produces mostly well-isolated nanowires and some nanoparticle aggregates. Electron microscope images obtained from many different samples illustrate that nanowire diameters range from 5 to 70 nm and that their lengths vary from a few hundred nanometers to tens of micrometers. The average length of nanowires was found to increase with the reaction time. Analysis of high-resolution TEM images shows that the nanowires are composed of crystalline $BaTiO_3$, in agreement with the X-ray diffraction analysis of nanowire ensembles. The convergent-beam electron diffraction (CBED) patterns shown in Figure 1b exhibit a sharp diffraction pattern consistent with a body-centered cubic structure with a lattice constant of ~ 4 Å. The diffraction patterns also show that a principal axis of the unit cell is aligned along the wire axis. The CBED patterns taken from different positions along the nanowire are found to be identical within experimental accuracy, demonstrating that the whole nanowire is single-crystalline. Extensive analyses of nanowire samples prepared from different reaction runs show that nearly all the nanowires exhibit the same crystalline behavior.

3. Scanning Probe Characterization

We probed the nanoscale ferroelectric properties of $BaTiO_3$ nanowires using a ultrahigh vacuum scanning probe microscope with a conductive tip.[22] Scanning probe microscopy
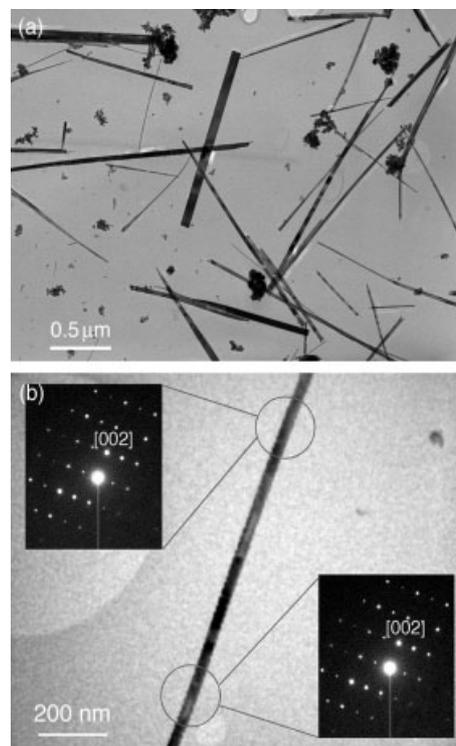

Fig. 1. a) TEM image of $BaTiO_3$ nanowires, showing that the reaction produces mainly nanowires and small quantities (~ 10 %) of nanoparticle aggregates. b) TEM image of a $BaTiO_3$ nanowire along with two convergent beam electron diffraction (CBED) patterns shown as insets. The circles represent the region where the CBED patterns are obtained. Analysis of the CBED patterns show that the nanowire is single crystalline with the [001] direction aligned along the wire axis.

(SPM) has emerged as one of the most valuable means of examining the properties of ferroelectric thin films and patterned nanostructures:[16,29–35] the topography of a sample can be studied with nanoscale resolution using SPM operating in an atomic force microscopy (AFM) mode, whereas the ferroelectric polarization can also be imaged and directly manipulated using electrostatic force microscopy (EFM). Compared to other characterization methods such as Raman scattering and X-ray diffraction, SPM has a distinct advantage because it can readily locate individual nanostructures, measure their sizes, and then directly probe and manipulate the ferroelectric polarization.

A schematic diagram illustrating the experimental geometry is presented in Figure 2a. To induce or "write" local electric polarization on a nanowire, a voltage (V_{tip}) is applied to the conductive tip while holding the tip at a fixed distance above the nanowire on a gold substrate. The written polarization is then probed or "read" using EFM by measuring the shift in the resonance frequency of a SPM cantilever while scanning it with small V_{tip}.[16,29–35] The attractive and repulsive electrostatic interactions between the tip and the nanowire change the resonance frequency of the cantilever in the opposite directions. A plot of the resonance frequency as a function of tip position therefore provides a spatial map of electric polarization directions on a nanowire.
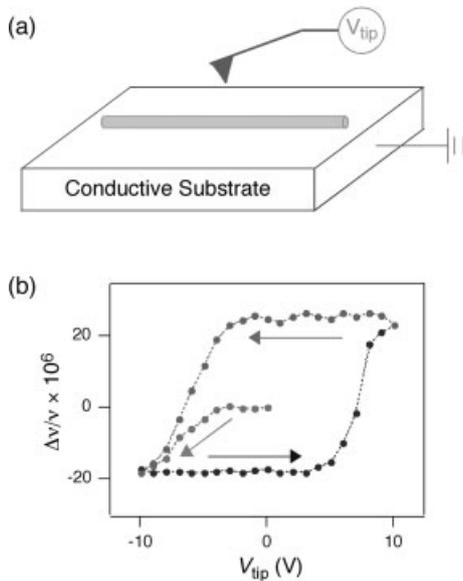
Fig. 2. a) Schematic diagram illustrating the experimental geometry for reading and writing local areas of polarization on a nanowire. b) Plot of the fractional shift in the cantilever resonance frequency ($\Delta v/v = (v_0 - v)/v_0$) as a function of the writing voltage (V_{tip}) that illustrates a hysteresis behavior of polarization switching. The electrostatic force felt by the tip and hence the magnitude of electric polarization on the nanowire is directly proportional to $\Delta v/v$. Each data point in the plot was obtained by applying the writing voltage for 3 min and subsequently measuring the shift in the cantilever resonance frequency at $V_{tip} = -2$ V. The V_{tip} scan sequence for writing was from 0 to –10 V (light gray), –10 V to +10 V (black), and +10 V to –10 V (dark gray). The distance between the tip and the top surface of the nanowire was 10 nm during the writing procedure and 35 nm during the reading procedure.

Figures 3a–d show successive EFM images of four distinct polarization domains written on a 12 nm diameter nanowire together with a topographic image, and they demonstrate that multiple nanoscale polarization domains can be independently induced and manipulated on a single $BaTiO_3$ nanowire. These EFM images are obtained by subtracting an image at
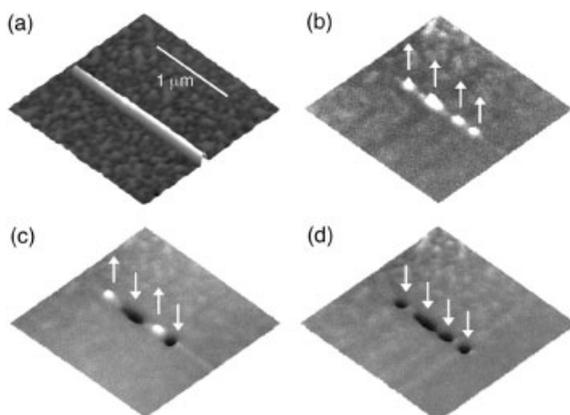

Fig. 3. a) Topographic image of a 12 nm diameter $BaTiO_3$ nanowire. b–d) Successive electrostatic force microscope (EFM) images showing that four distinct polarization domains can be independently manipulated by an external electric field. In these EFM images, the bright and dark colors correspond to the resonance frequency shift of +10 Hz and –10 Hz, respectively, and the white arrows indicate polarization directions. The upward and downward polarization spots were written with $V_{tip} = -10$ V and $V_{tip} = +10$ V, respectively, and the EFM images were obtained by subtracting an EFM image at $V_{tip} = +1.5$ V from that at $V_{tip} = -1.5$ V. The distance between the tip and the top surface of the nanowire was 10 nm during the writing procedure and 35 nm during the reading procedure.

$V_{tip} = +1.5$ V from that at $V_{tip} = -1.5$ V to eliminate the capacitive contribution between the tip and the nanowire. They therefore exhibit only the contribution from the surface charges associated with a local electric polarization. Pristine nanowires show no discernible EFM contrast, indicating that they do not exhibit polarization perpendicular to the wire axis. The EFM images obtained after the writing procedure with $V_{tip} = -10$ V and $V_{tip} = +10$ V clearly show, on the other hand, that a local electric polarization perpendicular to the wire axis can be induced by an external electric field. Investigations on many nanowires with different diameters show that the written polarization does not decay appreciably over a period exceeding seven days in an ultrahigh vacuum environment.

Close inspection of Figure 3 shows that an EFM spot induced by a tip fixed at a particular position is roughly circular in shape and that its size is ~30 nm, roughly the same as the distance between the tip and the nanowire surface during the reading procedure. Considering that the size of a polarization domain perpendicular to the wire axis is limited by the nanowire diameter, the circularity of EFM spots suggests that the spatial extent of the polarization along the nanowire length is comparable to the nanowire diameter, and hence nanoscale polarization domains as small as ~100 nm^2 in size can be induced on a nanowire.

The ferroelectric nature of a $BaTiO_3$ nanowire can be further probed using the hysteresis characteristics associated with local polarization reversal shown in Figure 2b. Specifically, Figure 2b shows that once the polarization perpendicular to the wire is created by an external field, its reversal exhibits a clear memory effect with a remanence-to-saturation ratio close to one. It further shows that the coercive electric field (E_c), at which the polarization changes its direction, is ~7 kV cm^{-1}, assuming that the relative dielectric constant of a $BaTiO_3$ nanowire is ~1200 as in bulk crystals.[36] Experiments on different nanowires show that the value of E_c remains roughly the same, irrespective of nanowire diameter in the range of 10–50 nm. This value of E_c compares favorably to E_c ~10 kV cm^{-1} determined from a bulk $BaTiO_3$ single crystal,[36] but it is smaller than typical E_c ~30 kV cm^{-1} in polycrystalline samples.[23] Since the E_c values are known to be sensitive to the presence of domain walls and defects,[23,37,38] the observed E_c of ~7 kV cm^{-1} demonstrates that $BaTiO_3$ nanowires are nearly free of defects.

4. Conclusions and Future Prospects

The availability of ferroelectric nanowires provides exciting new opportunities for studying nanoscale ferroelectricity, paraelectricity, and piezoelectricity. These nanowires are essentially single-crystalline and defect-free ferroelectrics. The synthetic method reported here can be applied to a variety of other perovskite material systems to address a range of open scientific and technological challenges. Also, the one-dimensional nature of nanowires allows for easy formation of different self-assembled structures, such as crossbar arrays, which

may prove useful in fabricating a variety of nanoscale functional devices. Furthermore, the work presented here demonstrates that the study of these nanowires using scanning probe microscopy represents a unique opportunity for investigating ferroelectricity in individual nanostructures.

[1] A. P. Alivisatos, *Science* **1996**, *271*, 933.
[2] J. Hu, T. W. Odom, C. M. Lieber, *Acc. Chem. Res.* **1999**, *32*, 435.
[3] M. Bockrath, W. J. Liang, D. Bozovic, J. H. Hafner, C. M. Lieber, M. Tinkham, H. K. Park, *Science* **2001**, *291*, 283.
[4] W. J. Liang, M. Bockrath, D. Bozovic, J. H. Hafner, M. Tinkham, H. Park, *Nature* **2001**, *411*, 665.
[5] A. M. Morales, C. M. Lieber, *Science* **1998**, *279*, 208.
[6] J. D. Holmes, K. P. Johnston, R. C. Doty, B. A. Korgel, *Science* **2000**, *287*, 1471.
[7] Y. Cui, C. M. Lieber, *Science* **2001**, *291*, 851.
[8] X. Duan, Y. Huang, Y. Cui, J. Wang, C. M. Lieber, *Nature* **2001**, *409*, 66.
[9] M. H. Huang, S. Mao, H. Feick, H. Q. Yan, Y. Y. Wu, H. Kind, E. Weber, R. Russo, P. D. Yang, *Science* **2001**, *292*, 1897.
[10] X. Peng, L. Manna, W. Yang, J. Wickham, E. Scher, A. Kadavanich, A. P. Alivisatos, *Nature* **2000**, *404*, 59.
[11] V. F. Puntes, K. M. Krishnan, A. P. Alivisatos, *Science* **2001**, *291*, 2115.
[12] C. R. Martin, *Chem. Mater.* **1996**, *8*, 1739.
[13] T. Thurn-Albrecht, J. Schotter, C. A. Kastle, N. Emley, T. Shibauchi, L. Krusin-Elbaum, K. Guarini, C. T. Black, M. T. Tuominen, T. P. Russell, *Science* **2000**, *290*, 2126.
[14] M. E. Lines, A. M. Glass, *Principles and Applications of Ferroelectrics and Related Materials,* Clarendon Press, Oxford **1977**.
[15] J. F. Scott, *Ferroelectr. Rev.* **1998**, *1*, 1.
[16] C. H. Ahn, T. Tybell, L. Antognazza, K. Char, R. H. Hammond, M. R. Beasley, O. Fischer, J. Triscone, *Science* **1997**, *276*, 1100.
[17] S. Mathews, R. Ramesh, T. Venkatesan, J. Benedetto, *Science* **1997**, *276*, 238.
[18] B. H. Park, B. S. Kang, S. D. Bu, T. W. Noh, J. Lee, W. Jo, *Nature* **1999**, *401*, 682.
[19] W. Y. Shih, W.-H. Shih, I. A. Aksay, *Phys. Rev. B* **1994**, *50*, 15 575.
[20] P. Ayyub, S. Chattopadhyay, R. Pinto, M. S. Multani, *Phys. Rev. B* **1998**, *57*, R5559.
[21] J. J. Urban, W. S. Yun, Q. Gu, H. Park, *J. Am. Chem. Soc.* **2002**, *124*, 1186.
[22] W. S. Yun, J. J. Urban, Q. Gu, H. Park, *Nano Lett.* **2002**, *2*, 447.
[23] H. B. Sharma, H. N. K. Sarma, *Thin Solid Films* **1998**, *330*, 178.
[24] C. Liu, B. Zou, A. J. Rondinone, Z. J. Zhang, *J. Am. Chem. Soc.* **2001**, *123*, 4344.
[25] D. L. Kaiser, M. D. Vaudin, G. Gillen, C.-S. Hwang, L. H. Robins, L. D. Rotter, *J. Cryst. Growth* **1994**, *137*, 136.
[26] B. W. Wessels, *Annu. Rev. Mater. Sci.* **1995**, *25*, 525.
[27] S. O'Brien, L. Brus, C. B. Murray, *J. Am. Chem. Soc.* **2001**, *123*, 12 085.
[28] C. B. Murray, D. J. Norris, M. G. Bawendi, *J. Am. Chem. Soc.* **1993**, 115, 8706.
[29] X. Q. Chen, H. Yamada, T. Horiuchi, K. Matsushige, S. Watanabe, M. Kawai, P. S. Weiss, *J. Vac. Sci. Technol. B* **1999**, *17*, 1930.
[30] C. Durkan, M. E. Welland, D. P. Chu, P. Migliorato, *Phys. Rev. B* **1999**, *60*, 16 198.
[31] C. Durkan, D. P. Chu, P. Migliorato, M. E. Welland, *Appl. Phys. Lett.* **2000**, *76*, 366.
[32] T. Tybell, C. H. Ahn, J.-M. Triscone, *Appl. Phys. Lett.* **1998**, *72*, 1454.
[33] T. Tybell, C. H. Ahn, J.-M. Triscone, *Appl. Phys. Lett.* **1999**, *75*, 856.
[34] S. V. Kalinin, D. A. Bonnell, *Appl. Phys. Lett.* **2001**, *78*, 1116.
[35] S. V. Kalinin, D. A. Bonnell, *Phys. Rev. B* **2001**, *63*, 125 411.
[36] G. A. Samara, *Phys. Rev.* **1966**, *151*, 378.
[37] A. M. Bratkovsky, A. P. Levanyuk, *Phys. Rev. Lett.* **2000**, *84*, 3177.
[38] A. M. Bratkovsky, A. P. Levanyuk, *Phys. Rev. Lett.* **2000**, *85*, 4614.